3. J. M. Matsen and B. L. Tarmy, *Chem. Eng. Prog. Symp. Ser. No. 101* (1970), p. 1.
4. D. Kunii and D. Levenspiel [*Fluidization Engineering* (Wiley, New York, 1969)] discuss failure of the scale-up of a hydrocarbon synthesis plant and other problems.
5. This is related to the behavior of magnetic stress in the medium, considered as a homogeneous magnetized continuum. A local perturbation in voidage modifies the uniform stress of the unperturbed bed, creating forces that restore the medium to the uniform state (R. E. Rosensweig, *Ind. Eng. Chem. Fundam.*, in press). For a treatment of the hydrodynamics of the growth of perturbations in conventional fluidized solids see T. B. Anderson and R. Jackson [*ibid.* **7**, (No. 1), 12 (1968)].
6. Previous investigators have apparently overlooked the sufficient role played by orientation and uniformity of the applied magnetic field [for example, D. G. Ivanov and G. T. Grozev, *C. R. Acad. Bulg. Sci.* **23** (No. 7) 787 (1970); and R. L. Sonoliker *et al.*, *Ind. J. Technol.* **10**, 377 (1972)]. In a uniform applied magnetic field the bed is free of any magnetic force, but previous workers have often attributed the delay of bubbling at higher flow rates to a magnetic force added to the force at gravity. More important as a distinguishing feature is the existence of the stabilized, levitated range reported here at velocities between μ_M and μ_T [R. E. Rosensweig, U.S. Patent No. 4,115,927 (1978)].
7. Measurements of a particulate sample with a vibrating sample magnetometer gave magnetization values of 372 G at an applied field of 5000 Oe, 326 G at 3000 Oe, 250 G at 1000 Oe, and 132 G at 200 Oe. The material is ferromagnetically soft with a remanence of less than 5 G.
8. As the flow rate of the gas is slowly increased to the vicinity of the transition point, the bed surface in some instances bubbles over part or all of its area for a limited time, then returns to the motionless state; apparently the medium adjusts to a new structure. An incremental increase in throughput then produces steady bubbling and is taken as the experimental transition point.
9. Particles comprising nickel supported on alumina that were crushed and sieved to the size range 0.177 to 0.250 mm formed a bed with a settled height after aeration of 14 mm. In the absence of applied magnetic field, surface bubbling occurred at a superficial velocity of 2.9 cm/sec. With application of a transverse magnetic field of 570 Oe, transition to bubbling was increased somewhat to 4.3 cm/sec. In an axially oriented field of 570 Oe the bed expanded quiescently to 20.0 cm/sec, where momentary bubbling occurred (transition with restructuring), followed by quiescent expansion to 29.0 cm/sec, where transition to steady bubbling was observed.
10. For the long, magnetically saturated beds U depends only on ρ, M, ϵ, g, and F where g is the gravitational constant and F is the fluid-particle drag force per unit volume of the emulsion. Dimensional reasoning simplifies the relationship to the interdependence among the three groups, $\rho U^2/M^2$, ϵ, and $F/\rho g$. The condition of fluidization is $(F/\rho g) = 1 - \epsilon$, so that $\rho U^2/M^2$ is uniquely related to the ϵ alone.
11. Experiments with electrofluidized beds are reported by T. W. Johnson and J. R. Melcher [*Ind. Eng. Chem. Fundam.* **14**, 146 (1975)], P. W. Dietz and J. R. Melcher [*ibid.* **17**, 112 (1978)], G. M. Colver [*Powder Technol.* **17**, 9 (1977)], and others. There should be parallels to the magnetic stabilization, although these investigators focused on particulate collection in turbulent beds and the influence of the electric field on bubble dynamics. There seems to be no indication that electrically calmed beds are flowable. Polarization forces developed in electric fields are not as strong as those that can be developed in magnetic fields, while the existence of free charge in such beds has no analog in the magnetic case.
12. Discharge coefficient was calculated from

$$C = \frac{L^{1/2} - L_o^{1/2}}{(g/2)^{1/2}} \frac{1}{T} \left(\frac{d_b}{d_o}\right)^2$$

where L is initial depth over orifice center, L_0 the depth after time T, d_b the bed diameter, d_o orifice diameter, and g the gravitational constant (980 cm/sec^2). For the system in Fig. 2F, L is 8 to 14 cm, and L_0 is 4 cm; d_b is 7.37 cm (inner diameter), d_o = 0.83 cm, and gas superficial velocity, 15.6 cm/sec.
13. I thank J. J. Schlaer for his invaluable help in carrying out the experiments.

18 September 1978; revised 4 December 1978

Interplanetary Magnetic Field Polarity and the Size of Low-Pressure Troughs Near 180°W Longitude

Abstract. *When the interplanetary magnetic field is directed away from the sun, the area of wintertime low-pressure (300-millibar) troughs near 180°W longitude is significantly larger than when the field is toward the sun. This relation persists during most of the winters of 1951 to 1973.*

Low-pressure (300-mbar) troughs (cyclones) that are near 180°W longitude when the interplanetary magnetic field is directed away from the sun are, on the average, significantly larger than when the field is toward the sun. The difference in area persists during a 5-day interval in which the troughs move from 180°W to the North American continent. This relation persists during most of the winters from 1951 to 1973. (The winter of 1951 is defined as October 1950 through March 1951.)

Roberts and Olson (*1*) reported that troughs that cross 180°W 2 to 4 days after an increase in geomagnetic activity tend to become significantly larger than average. The size of the troughs was measured by using the vorticity area index (VAI), which is defined as the area of the trough where the absolute vorticity (circulation per unit area) at 300 mbar exceeds a value of 20×10^{-5} sec^{-1} plus the area where the vorticity exceeds 24×10^{5} sec^{-1}. These vorticity values correspond to a well-formed trough. The VAI was recorded for a trough on the first day after it had crossed 180°W during the course of its eastward motion (occasionally a trough was formed east of 180°W and was similarly counted). After a trough had been identified east of 180°W, its VAI was measured twice a day for the next 12 days (during some winters the area was recorded for only the first 3 days and during some early years data were available only once a day). In the study reported here we used the same measurements of trough area that were used by Roberts and Olson (*1*); however, in the present study there is no reference to the times of sector boundary passages (and therefore to times of varying geomagnetic activity), so the results reported here are not directly comparable to those of Roberts and Olson. In some of our earlier work (*2*) the VAI summed over all troughs in the entire

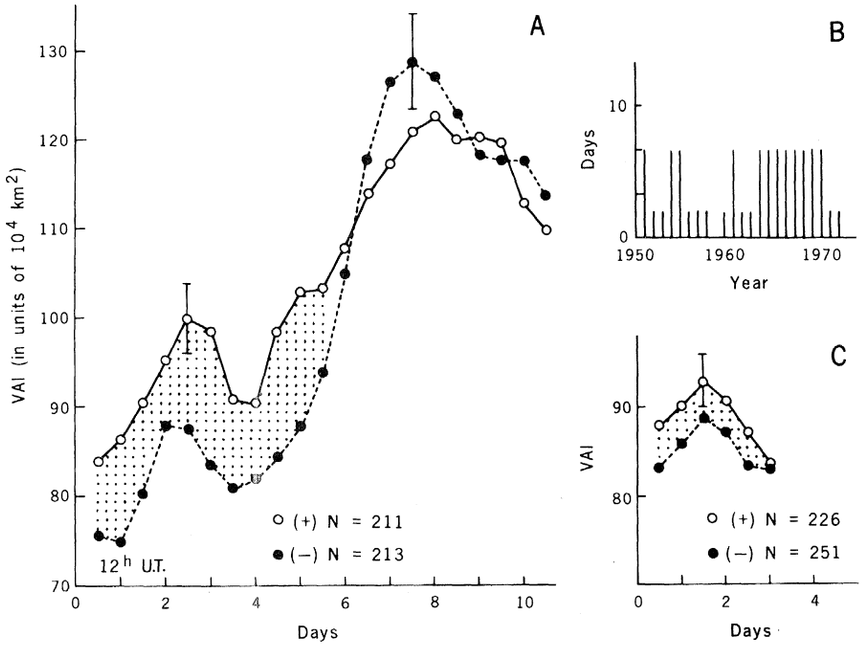

Fig. 1. (A) Average area of low-pressure troughs (cyclones) during the 10 days after the troughs crossed 180°W: (○) away troughs and (●) toward troughs (see text for explanation). During the first 5 days after the troughs crossed 180°W, the area of the away troughs is significantly larger than the area of the toward troughs. Error bars are plus or minus the standard error of the mean. (B) Indication of winters during which trough area data were available for 10 days after the troughs crossed 180°W and of winters during which the data were available for only 3 days. (C) Same as first 3 days in (A) but computed for years in which trough area data were available for only 3 days. The area of the away troughs is again larger than the area of the toward troughs.

0036-8075/79/0406-0060$00.50/0

Northern Hemisphere north of 20°N was used. This approach was useful in defining the significance of the results (*3*), but for understanding the physical mechanisms the present approach of studying individual troughs may be more useful.

Figure 1A shows the result of dividing the wintertime troughs near 180°W into two groups. The "away" troughs are those for which the interplanetary magnetic field was directed away from the sun on the day when the trough was first identified east of 180°W. The average VAI of these away troughs during each of the next 10 days is shown in Fig. 1A. The "toward" troughs are similarly defined. The direction of the interplanetary field was obtained from Svalgaard's atlas (*4*). Day zero is the day on which the troughs were first identified east of 180°W. Figure 1A shows that on day zero the average area of the away troughs was significantly larger than the area of the toward troughs and that this difference in area persisted for 5 days during which the troughs moved to the North American continent.

Figure 1A was prepared by using trough observations during the 12 winters for which data out to at least 10 days after day zero were available, as indicated in Fig. 1B. During most of the other winters in the interval 1951 to 1973 data were available for only the first 3 days after day zero. Figure 1C shows that the same excess area associated with away troughs was found when these winters were analyzed separately.

We suggest that a physical cause of the larger area of away troughs may be associated with the topological fact that an interplanetary magnetic field line from the sun with away polarity can merge with a geomagnetic field line from the northern polar region of the earth, while an interplanetary magnetic field line from the sun with toward polarity can merge with the geomagnetic field line from the southern polar region of the earth. Thus energetic particle fluxes from the sun will have ready access to the northern polar region when the interplanetary field is away from the sun and to the southern polar region when the field is toward the sun. Yeager and Frank (*5*) observed that the flux of solar electrons with energies of a few hundred electron volts on magnetic field lines connected to the northern polar cap is an order of magnitude larger when the interplanetary field is away from the sun than when it is toward the sun. We do not suggest that this particular electron flux is the cause of the trough area effect, but the results of Yeager and Frank dramatically illustrate the influence of the direction of the interplanetary magnetic field on solar particle fluxes entering the northern polar region of the earth.

The relation reported here is sturdy. It persists when the data set is divided into two parts by using the first half and last half of the data or by using every other trough in sequential order. The resulting four graphs are very similar to Fig. 1A and so are not shown here.

The persistence of the relationship through most of the winters of 1951 to 1973 is shown in Fig. 2A. For each winter in this interval the number of months in which the away troughs had a larger area and the number of months in which the toward troughs had a larger area are indicated. Figure 2A shows that in most of the individual winters there were more months during which the away sectors were larger. Figure 2B shows the combined distribution during all the winters shown in Fig. 2A. The distribution representing away polarity is clearly considerably separated from the distribution representing toward polarity.

Another test of the significance of the relationship is shown in Fig. 3. The analysis that led to Fig. 1A was repeated, but a different day (with respect to the day on which the troughs crossed 180°W) was used for classifying the troughs as away or toward. In Fig. 3A the abscissa is the day on which the troughs were classified as away or toward, and the ordinate is the average difference between the area of the away troughs and the area of the toward troughs during the first 5 days after day zero (corresponding to the dotted portion of Fig. 1A). Thus the point for day zero in Fig. 3A corresponds

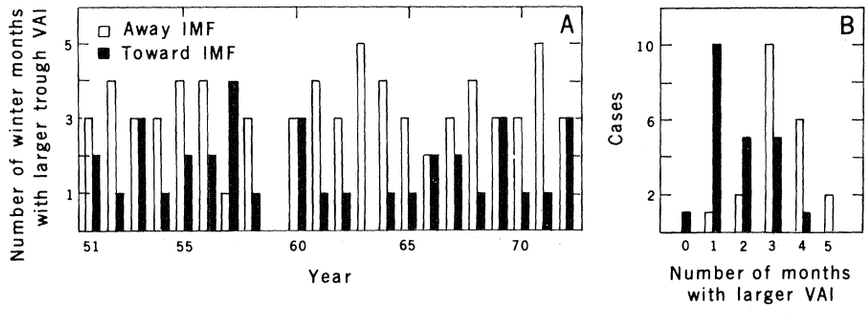

Fig. 2. (A) Number of months in the winters of 1951 to 1973 (except 1959, for which no data were available) in which the away troughs (open bars) had a larger area and toward troughs (shaded bars) had a larger area. Away troughs had larger area during more months than toward troughs in almost all these winters. The first 3 days after day zero were used. (B) Distribution of number of months in which away troughs (open bars) had a larger area and toward troughs (shaded bars) had a larger area during all the winters examined. The distribution of open bars is centered at a larger number and is well separated from the distribution of shaded bars.

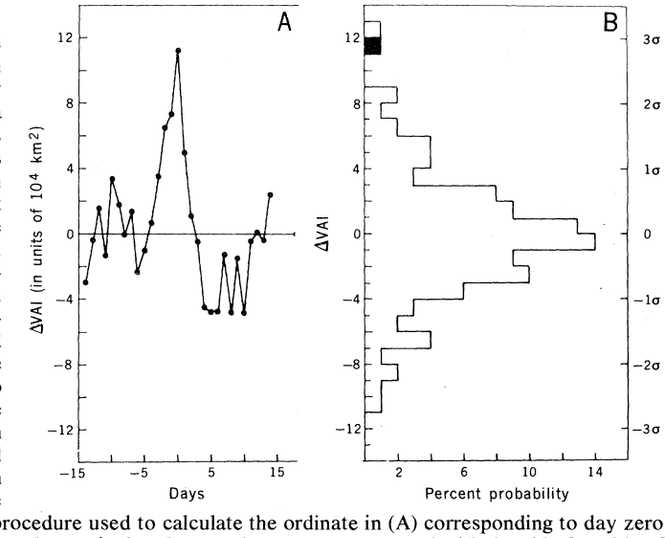

Fig. 3 (A) Average difference between the area of away troughs and the area of toward troughs during the first 5 days of the time scale in Fig. 1A plotted against the day on which the troughs were classified as away or toward according to the observed direction of the interplanetary magnetic field on that day. Thus the point corresponding to day zero is the average difference between the open circles and the closed circles in Fig. 1A during the first 5 days. (B) The procedure used to calculate the ordinate in (A) corresponding to day zero was repeated 1000 times, but assigning the troughs as away or toward with the aid of a table of random numbers. This shows the probability of obtaining a given value of the ordinate in (A) by chance. (■) Observed value of the ordinate in (A) at day zero. On the right ordinate σ is the standard error of the mean. The calculated result in (A) is thus about 3σ away from a null result.

to the average difference of the two curves in Fig. 1A during the first 5 days. The peak at day zero in Fig. 3A suggests that the relationship described here between the interplanetary field polarity and the size of low-pressure troughs is most effective in the geographic area corresponding to day zero, that is, near 180°W. We are making a new data set to define this geographic area and to search for other possible similar areas such as the Icelandic low.

Figure 3B shows a distribution of 1000 calculations of the ordinate value but with the troughs assigned as away or toward by using a random number generator. The excess areas of away troughs calculated by using the observed direction of the interplanetary magnetic field was equaled in magnitude during less than 1 percent of the random calculations. On the right-hand scale of Fig. 3B, σ represents the standard error of the mean. The observed relationship is about three standard errors removed from a null result.

The relationship reported here has led us to devise an improved data set describing the area of low-pressure troughs. We plan to identify each trough when it first appears in the Northern Hemisphere and then at 12-hour intervals to record the time, latitude, and longitude of the central portion of the trough, the VAI computed with several values of vorticity, and other related quantities such as the maximum value of vorticity within the trough. The limitation in the present data set to wintertime troughs near 180°W will thus be removed. It should be possible to define the geographic area in the Northern Hemisphere in which this relationship exists.

J. M. WILCOX, P. B. DUFFY*
K. H. SCHATTEN, L. SVALGAARD
P. H. SCHERRER
Institute for Plasma Research, Stanford University, Stanford, California 94305
W. O. ROBERTS
R. H. OLSON
Aspen Institute for Humanistic Studies, Boulder, Colorado 80302

References and Notes

1. W. O. Roberts and R. H. Olson, *J. Atmos. Sci.* **30**, 135 (1973); *Rev. Geophys. Space Phys.* **11**, 731 (1973).
2. J. M. Wilcox, P. H. Scherrer, L. Svalgaard, W. O. Roberts, R. H. Olson, *Science* **180**, 185 (1973); J. M. Wilcox, P. H. Scherrer, L. Svalgaard, W. O. Roberts, R. L. Jenne, *J. Atmos. Sci.* **31**, 581 (1974); J. M. Wilcox, L. Svalgaard, P. H. Scherrer, *Nature (London)* **255**, 539 (1975); *J. Atmos. Sci.* **33**, 1113 (1976); J. M. Wilcox, *Science* **192**, 745 (1976).
3. C. O. Hines and I. Halevy, *Nature (London)* **258**, 313 (1975); *J. Atmos. Sci.* **34**, 382 (1977).
4. J. M. Wilcox, L. Svalgaard, P. C. Hedgecock, *J. Geophys. Res.* **80**, 3685 (1975); L. Svalgaard, "Interplanetary sector structure 1947-1975," *Stanford Univ. Inst. Plasma Res. Rep. 648* (1976).
5. D. M. Yeager and L. A. Frank, *J. Geophys. Res.* **81**, 3966 (1976).
6. Work at Stanford was supported by the Office of Naval Research under contract N00014-76-C-0207, the National Aeronautics and Space Administration under grant NGR 05-020-559, the Atmospheric Sciences Section of the National Science Foundation under grants ATM77-20580 and DES75-15664, and the Max C. Fleischmann Foundation; work at the Aspen Institute for Humanistic Studies was supported by the Department of Energy under contract ER-78-02-4634.000.
* Present address: Center for Astrophysics, Harvard University, Cambridge, Mass. 02138.

7 September 1978; revised 18 December 1978

Spectral Analysis of Zooplankton Spatial Heterogeneity

Abstract. *Continuous estimates were obtained of zooplankton abundance, chlorophyll fluorescence, and water temperature along 10- to 100-kilometer transects of the North Sea. Spectral analysis methods were applied to the data. The "patchiness" of the plankton was distributed over all the length scales resolved with no indication of a characteristic patch size. The relative intensity of the zooplankton patchiness was greater than that of the phytoplankton at all spatial scales, with this difference becoming progressively greater for finer-scale features. In the North Sea data, the concentrations of phytoplankton and zooplankton consistently showed negative spatial correlations.*

Considerable interest, both theoretical and experimental, has been focused on spatially heterogeneous biological systems. In large part this interest stems from studies showing that spatial heterogeneity is probably both caused by and contributory to the complex nonlinear dynamic behavior of such systems (*1*). Planktonic systems are particularly useful for experimental observation because the physical structure of the pelagic environment is both relatively weak and transitory in time; persistent biological structure is likely to reflect biological causation at some spatial scale.

Several authors (*2*) have employed time series (spectral) analysis methods in descriptive studies of phytoplankton patchiness. The advantage of these methods is that they allow the variance and covariance of serial data to be resolved into component length scales; their disadvantage is that they require long series of closely spaced samples. Chlorophyll fluorescence in vivo provides an appropriate method for estimating phytoplankton concentration (*3*), but until recently there has not been a method comparable in resolution and potential transect length for estimating zooplankton abundance.

We have developed a shipboard sampling system which counts individual particles in a continuous stream pumped from a fixed-depth seawater intake. The particle counter senses the increased resistances resulting from the passage of particles between the sensor electrodes (*4*, *5*). As configured for the work reported here, the system does not discriminate particle size but simply counts the particles larger than threshold size (determined by a sigmoid sensitivity curve centered at 0.375-mm spherical equivalent diameter) and smaller than the sensing tubes (roughly 4-mm equivalent diameter). In all the regions we have sampled, this size range is numerically dominated by small crustacean zooplankton. For the transect reported here, visual counts of concurrent samples collected at the drain of the system showed the population to be composed almost exclusively (~ 95 percent) of copepods of the genera *Calanus*, *Oithona*, and *Pseudocalanus*. A calibration curve of visual versus electronic counts is given in Fig. 1.

The sampling system also obtains simultaneous records of chlorophyll fluorescence (measured with a Turner Designs fluorometer) and water temperature. Because it is immune to the problem of net clogging, the system al-

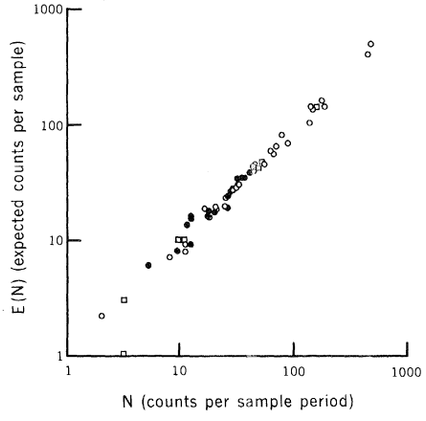

Fig. 1. Expected counts (visual counts of calibration samples weighted by a measured curve of particle size versus counting efficiency) plotted against electronic pulse counts from the sampling system. (●) Laboratory samples, (○) field samples, and (□) samples collected from the Dalhousie University 70-m³ "tower tank."

0036-8075/79/0406-0062$00.50/0